Efficient simulation of multi-dimensional detonation phenomena

Ralf Deiterding

Chair of Numerical Mathematics & Scientific Computing
Institut of Mathematics, Technische University Cottbus
Germany
deiterding@math.tu-cottbus.de
http://www.math.tu-cottbus.de/~deiter

Generalized Euler equations

The computation of inviscid flows with chemical reaction requires the usage of generalized Euler equations. In cartesian coordinates the following equations have to be applied:

K continuity equations for K different gaseous species:

$$\partial_t \rho_i + \sum_{n=1}^{N} \partial_{x_n}(\rho_i v_n) = \dot{m}_i \qquad \text{for } i = 1,\ldots,K$$

N momentum equations:

$$\partial_t(\rho v_m) + \sum_{n=1}^{N} \partial_{x_n}(\rho v_n v_m + \delta_{n,m}\, p) = 0 \qquad \text{for } m = 1,\ldots,N$$

Energy equation:

$$\partial_t(\rho E) + \sum_{n=1}^{N} \partial_{x_n}\left[v_n(\rho E + p)\right] = 0$$

Equation of state

The species are assumed to be ideal gases in thermal equilibrium. The ideal gas law and Dalton's law can be applied:

$$p(\boldsymbol{\rho}, T) = \sum_{i=1}^{K} p_i = \sum_{i=1}^{K} \rho_i \frac{\mathcal{R}}{W_i} T = \rho \frac{\mathcal{R}}{W} T \qquad \text{with} \quad \rho = \sum_{i=1}^{K} \rho_i$$

Ideal gases are *thermally perfect* and the specific heats are functions of the temperature:

$$c_{pi} = c_{pi}(T) \quad , \qquad c_{vi} = c_{vi}(T) \quad , \qquad \gamma_i(T) = c_{pi}(T) \,/\, c_{vi}(T)$$

Caloric equation:

$$h(\boldsymbol{\rho}, T) = \sum_{i=1}^{K} Y_i h_i(T) \quad \text{mit} \quad h_i(T) = h_i^0 + \int_0^T c_{pi}(s)ds$$

Evaluation of $p(\boldsymbol{\rho}, T)$ requires the computation of $T = T(\boldsymbol{\rho}, e)$ from the implicit equation:

$$\sum_{i=1}^{K} \rho_i\, h_i(T) - \mathcal{R}T \sum_{i=1}^{K} \frac{\rho_i}{W_i} - \rho e = 0$$

Only in the case of *calorically perfect* gases with c_{pi}, c_{vi} const. $\Rightarrow \gamma = \gamma(\boldsymbol{\rho})$ the temperature T can be eliminated and an explicit equation of state can be derived:

$$p(\boldsymbol{\rho}, e) = (\gamma(\boldsymbol{\rho}) - 1)\left(\rho e - \sum_{i=1}^{K} \rho_i h_i^0\right)$$

Detailed chemistry

The chemical production rates $m_i(\rho_1,\ldots,\rho_K,T)$ are derived from a *reaction mechanism* that consists of M chemical reactions:

$$\sum_{i=1}^{K} \nu_{ji}^f S_i \rightleftharpoons \sum_{i=1}^{K} \nu_{ji}^r S_i \qquad\qquad j = 1,\ldots,M$$

The forward reaction rate $k_j^f(T)$ is calculated with an empirical Arrhenius law:

$$k_j^f(T) = A_j T^{\beta_j} \exp(-E_j/\mathcal{R}T)$$

Backward reaction rates are experimentally measured or calculated from the equilibrium constant $K_j^c(T)$ as $k_j^r(T) = k_j^f(T)/K_j^c(T)$.

Mass production rate of specie S_i:

$$\dot{m}_i = W_i \sum_{j=1}^{M} (\nu_{ji}^r - \nu_{ji}^f)\left[k_j^f \prod_{n=1}^{K}\left(\frac{\rho_n}{W_n}\right)^{\nu_{jn}^f} - k_j^r \prod_{n=1}^{K}\left(\frac{\rho_n}{W_n}\right)^{\nu_{jn}^r}\right] \qquad i = 1,\ldots,K$$

ZND detonation model

The simplified ZND detonation model is used to validate different numerical schemes. It is derived by assuming a stationary detonation wave with only one single irreversible reaction $A \longrightarrow B$ with normalized energy release $q_0 = -\Delta h^0$ and forward reaction rate $k^f(T) = \exp(-E^+/T)$.

Mass production rate of species A and B:

$$\dot{m}_A = -\rho_A \exp(-E^+/T)\,, \qquad \dot{m}_B = -\dot{m}_A$$

A and B are treated as calorically perfect gases with $\gamma_A = \gamma_B$. The equation of state therefore reads:

$$p(\boldsymbol{\rho}, e) = (\gamma - 1)\,(\rho e - \rho_A\, q_0)$$

The parameter $f = (D/D_{CJ})^2 \geq 1$ measures the degree of overdrive for a given ZND detonation traveling with speed D in respect to the minimal detonation velocity D_{CJ}. f determines the stability of a ZND wave.

Numerical Methods

Incorporation of source terms and extension to multiple dimensions via the method of fractional steps:

A sequence of N one-dimensional initial value problems for the homogeneous transport equations and the system of ordinary differential equations

$$\partial_t \rho_i = \dot{m}_i\,(\rho_1,\ldots,\rho_K,T) \qquad i = 1,\ldots,K$$

are solved successively within each time-step.

The following upwind schemes are employed to solve the homogeneous 1D transport equations:

- Godunov's method
- Roe's method with entropy correction only in sonic rarefactions (Roe) and with entropy enforcement by adding numerical viscosity (RoeV)
- Steger-Warming and van Leer's flux vector splitting methods
- Harten, Lax, van Leer's (HLL) method

Decoupled source term integration:

- Standard ODE-methods, e.g. semi-implicit Rosenbrock-Wanner method for stiff ODE's (detailed chemistry).
- Automatic stepsize adjustment allows an efficient treatment of source terms that involve time scales that are smaller than the global time-step.

Unstable ZND detonation

By applying an ODE solver of higher order different 1st order upwind schemes within the fractional-step method can be evaluated.

Linearized stability analysis for ZND waves predicts one unstable mode for $1.57 < f < 1.73$ and $\gamma = 1.2$, $E^+ = 50$, $q_0 = 50$. Starting from the unperturbed exact solution the numerical scheme should reproduce the unstable behavior.

$10\ pts/L_{1/2}$, $CFL = 0.9$

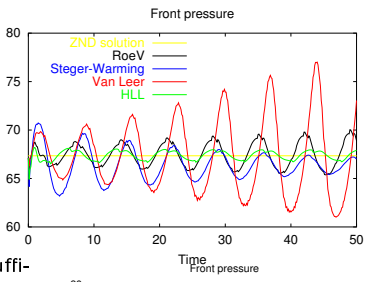

1. The instability is reproduced best with Van Leer's FVS. RoeV shows the unstable mode slightly. Steger-Warming FVS and HLL are to dissipative to resolve the detonation sufficiently at this resolution and do not reproduce the instability (upper right picture).

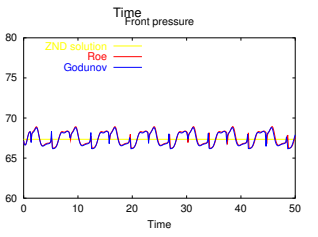

2. Numerical instabilities totally suppress the physical one when using Roe's or Godunov's method (lower right picture). $\longrightarrow$ The upwind scheme has to be sufficiently dissipative to stabilize the splitting method!

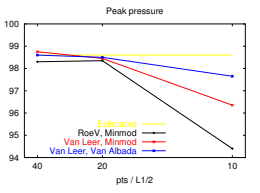

3. Higher order reconstruction technics within the upwind scheme can improve the solution significantly. (Compare maximal front pressures obtained with 2nd order MUSCL-Hancock in left picture to 1st order results).

Occurrence of the carbuncle phenomenon

If a one-dimensional upwind scheme is used to solve the multidimensional Euler equations on a structured grid with a fractional-step method, strong shock or typical detonation wave solutions may become unstable. Sufficient crossflow dissipation is necessary to stabilize the solution.

Van Leer, Steger-Warming, HLL, RoeV

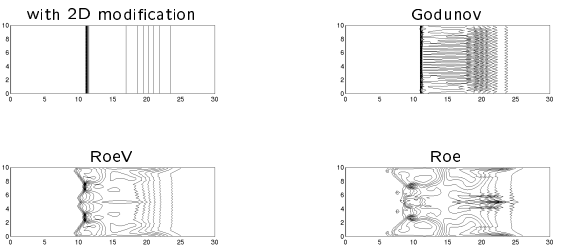

Isolines of density at $t = 10$ for different 1st order schemes (CFL=0.5)

Blockstructured AMR

A locally high resolution, which is essential for the accurate computation of detonation waves, is achieved by utilizing the most efficient adaptive method for hyperbolic conservation laws on blockstructured grids: The Berger and Oliger AMR algorithm.

+ Discretization necessary only for a single logically rectangular grid
+ Spatial *and* temporal refinement, no global time step restriction
+ No neighboring cell information has to be stored
+ Efficient cache reuse and vectorization possible
+ Simple load balancing
- Appropriate only for simple geometries
- Cluster algorithm necessary for grid generation
- Hanging nodes unavoidable and require special treatment
- Complex implementation

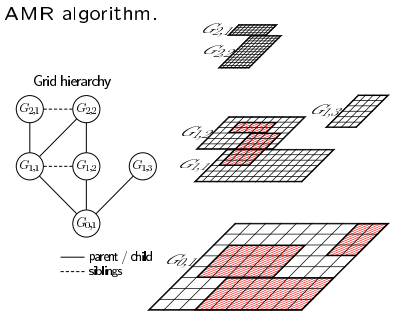

The blockstructured refinement strategy creates a hierarchy of properly nested subgrids.

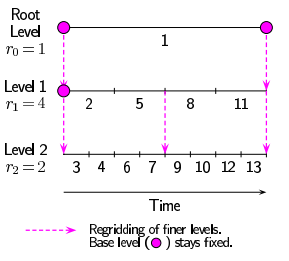

IntegrateLevel(l)

Repeat r_l times
  Set ghost cells of level l at time t
  If (time to regrid?) Then
    Regrid(l)
  Step Δt_l on all grids at level l
  If (level $l+1$ exists?) Then
    Set level l ghost cells at $t + \Delta t_l$
    IntegrateLevel($l+1$)
    Average level $l+1$ grids onto level l

AMR-algorithm and its recursive integration procedure. Refinement factor on level l is $r_l = \Delta t_{l-1}/\Delta t_l$.

A generic and flexible framework for AMR has been developed. It consists of three abstraction levels:

1. Specific application and numerical scheme.
2. AMROC (Adaptive Mesh Refinement in Object-oriented C++).
3. Parallel hierarchical data structures that employ the MPI-library.
   - Data follows "floor plan" of a single Grid Hierarchy.
   - Data of all levels resides on the same node $\rightarrow$ Most AMR operations are strictly local.
   - Neighboring grids are synchronized transparently even over processor borders when boundary conditions are applied.
   - Distribution algorithm: Generalization of Hilbert's space-filling curve

Typical benchmarks show high parallel efficiency and a performance like purely Fortran-based codes. Homepage: *http://www.math.tu-cottbus.de/~deiter/amroc*

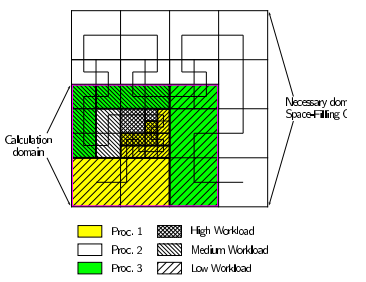

Construction of generalized Hilbert space-filling curve.

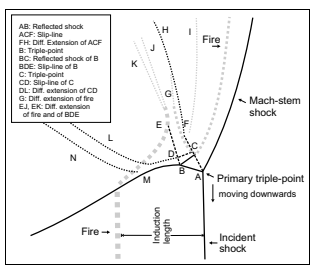

Schematic diagram of the flow around a triple-point.

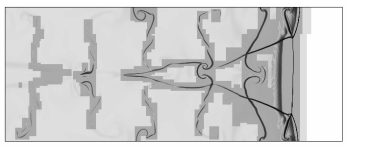

Dynamic adaption of the detonation wave.

Planar detonation with transverse waves

Experiments have shown that self-sustaining detonation waves are locally multidimensional and nonsteady. Triple-points form, which enhance the local chemical reaction significantly. Equilibrium-configurations with regular detonation cells are possible in particular cases.

- 34 elementary reactions for the 9 *thermally perfect* species H, O, OH, H_2, O_2, H_2O, HO_2, H_2O_2,Ar.
- Stoichiometric H_2-O_2-system with 70% Ar, at 6.7 kPa and 298 K.
- $\approx$ 22-44 cells within induction length.
- Adaption criteria:
  1. Scaled gradients $|Q_{i+1}^n - Q_i^n|$ of p and ρ
  2. Estimation of error in Y_i by Richardson extrapolation

The time history of the released chemical energy shows the detonation cells.

$$Q^n \overset{\Delta t, \Delta x}{\Longrightarrow} \tilde{Q} \qquad Q^{n-1} \overset{2\Delta t, 2\Delta x}{\Longrightarrow} \bar{Q} \qquad \tau = \frac{|\tilde{Q} - \bar{Q}|}{2^{d+1} - 2}$$

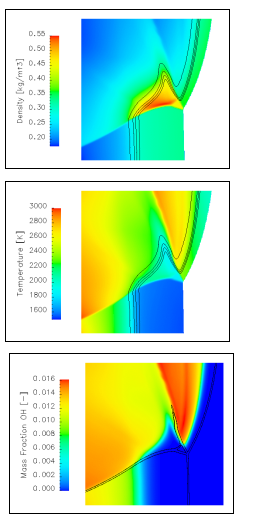

Detailed study of the flow around a triple-point. Additional isolines show the induction length.

Detonation with transverse and slapping waves

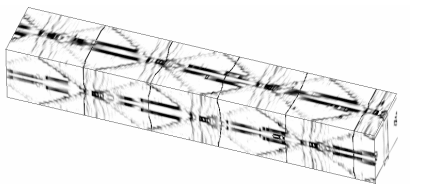

The time history of the vorticity shows regular orthogonal detonation cells.

- Quasi-stationary computation. Symmetric in y-direction.
- $\approx$ 16.8 cells within induction length.
- Adaptive computation uses 1.0M-1.5M cells. (Nonadaptive 8.8M). 80h real time on 48 PC-nodes.

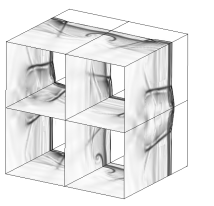

$t = 660\ \mu$s

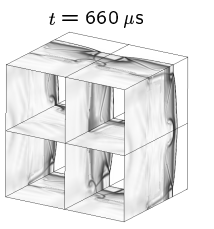

$t = 700\ \mu$s

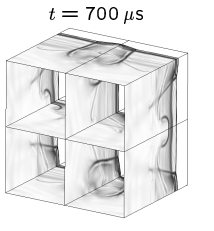

$t = 740\ \mu$s

Isolines of density on refinement grids for $t = 660\,\mu$s. Left pictures: Schlieren-plots of density.

Mach-reflection of a detonation wave

- Angle of inflow: 30^o
- $\approx$ 25 cells within induction length.
- Adaptive computation uses 470 k – 1 M cells. (Nonadaptive 59 M)
- 80h real time on 15 PC-nodes.

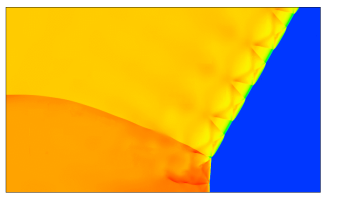

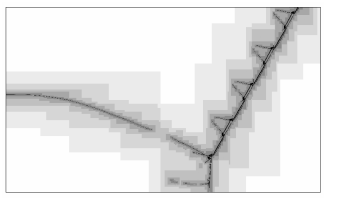

Left: Temperature distribution after $48\,\mu$s. Right: Adaption of detonation front and reflected shock.

Processor 1 Processor 2

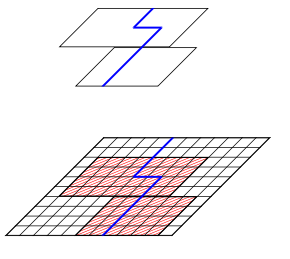

All higher level data follow the distribution of the base level.